optica

Kramers–Kronig coherent receiver

ANTONIO MECOZZI,[1,*] CRISTIAN ANTONELLI,[1] AND MARK SHTAIF[2]

[1]Department of Physical and Chemical Sciences, University of L'Aquila, L'Aquila 67100, Italy
[2]Department of Physical Electronics, Tel Aviv University, Tel Aviv 69978, Israel
*Corresponding author: antonio.mecozzi@univaq.it

The interest for short-reach links of the kind needed for inter-data-center communications has fueled in recent years the search for transmission schemes that are simultaneously highly performing and cost effective. In this work we propose a direct-detection coherent receiver that combines the advantages of coherent transmission and the cost-effectiveness of direct detection. The working principle of the proposed receiver is based on the famous Kramers–Kronig (KK) relations, and its implementation requires transmitting a continuous-wave signal at one edge of the information-carrying signal spectrum. The KK receiver scheme allows digital postcompensation of linear propagation impairments and, as compared to other existing solutions, is more efficient in terms of spectral occupancy and energy consumption. © 2016 Optical Society of America

1. INTRODUCTION

Coherent optical transmission schemes are optimal from the standpoint of spectral efficiency, as they allow the encoding of information in both quadratures and polarizations of the electric field. However, while they constitute the solution of choice for medium-to-long-reach applications, the cost of a coherent receiver is a major obstacle in the case of short-reach links, whose role in many areas of application is becoming increasingly important. Indeed, coherent receivers used today are based on the intradyne scheme, which requires two optical hybrids and four pairs of balanced photodiodes, making its overall cost unacceptably high for short links, such as those intended for inter-data-center communications. In recent years, the need for low-cost solutions has led to a number of simpler, direct-detection-based, transmission schemes [1]. Most common is the pulse-amplitude modulation (PAM) scheme, which relies on the transmission of pulses of several amplitudes. Another popular approach is that of direct-detection orthogonal frequency-division multiplexing (OFDM) [2,3] [also referred to as digital multitone (DMT)], where the OFDM tones are constrained to be symmetric with respect to the center frequency (for the signal to be real-valued), and where a bias is introduced so as to prevent signal negativity. A shortcoming of the above two methods is that they are not tolerant to linear propagation effects, primarily chromatic and polarization-mode dispersion. To resolve this issue, Lowery and Armstrong proposed the self-coherent heterodyne scheme [4,5], where a frequency offset local oscillator (LO) is launched into the system together with the signal, thereby allowing full reconstruction of the complex-valued field by means of direct detection. This approach allows the elimination of linear propagation impairments by using standard digital signal processing (DSP), but it also involves two

important disadvantages. First, the power budget becomes less favorable, as a notable fraction of the launched power needs to be allocated to the LO. Second, in order to avoid interference, the LO must be separated from the data-carrying signal by a frequency gap that is at least as large as the signal's bandwidth, thereby resulting in a reduction of the spectral efficiency by at least a factor of 2. A scheme that avoids the frequency gap was proposed by Schuster et al. [6]. However, the higher spectral efficiency is achieved at the expense of flexibility, because this scheme, unlike the self-coherent heterodyne scheme, does not allow digital compensation of linear propagation impairments, and is thereby mainly suited for short-range OFDM-based transmission systems. More recently, another single-sideband modulation/direct-detection scheme, which in principle is capable of full-field reconstruction, has been reported in [7].

In this paper we introduce a communication scheme that we call the self-coherent Kramers–Kronig (KK) method [8]. Our scheme consists of the same optical building blocks as the ones used in the scheme of Lowery and Armstrong [4,5], but, similarly to [6] and [7], it eliminates the need for a frequency gap between the LO and the signal and, hence, increases the spectral efficiency by a factor of 2 in comparison with that scheme. The extraction of the received complex-valued signal from the photocurrent is performed digitally while taking advantage of the KK relations between the phase and amplitude of the field impinging upon the photodiode, thereby justifying our choice for the scheme's name. The KK relations are somewhat ubiquitous, as they emerge in various areas of physics and engineering [10–14]. Their applicability in the context of direct-detection coherent receivers follows from a simple property of minimum phase signals, as discussed in [15,16]. Unlike the method of [6], the proposed

scheme allows the full reconstruction of the complex envelope of the optical field impinging upon the receiver, and hence it is compatible with DSP-based digital compensation of propagation-induced linear impairments. The gain in spectral efficiency comes at the expense of a somewhat more stringent requirement on the power of the transmitted LO tone in comparison with the self-heterodyne scheme. Nonetheless, as we show in what follows, in practical scenarios this power requirement can be considerably relaxed. We show that the proposed KK scheme is optimal in terms of information capacity with respect to the class of band-limited systems whose receivers are constrained to detect only the signal's intensity. Finally, we note that the methods that we discuss here are of relevance to the broader topic of phase reconstruction that has been attracting significant interest in many areas of optics [17].

2. MINIMUM PHASE SIGNALS

The communications scheme presented in this paper relies on identifying a condition that ensures that the received signal is minimum phase, in which case its phase can be uniquely extracted from its intensity. We denote by $s(t)$ a complex data-carrying signal whose spectrum is contained between $-B/2$ and $B/2$, and consider a single sideband signal of the form

$$h(t) = A + s(t) \exp(-i\pi Bt), \qquad (1)$$

where A is a constant. As described in [16], the Nyquist stability criterion [18] can be used to prove that $h(t)$ is a minimum phase signal if and only if the winding number of its time trajectory in the complex plain is zero (which in practice means that it does not encircle the origin). The illustration in Fig. 1 shows that this condition is satisfied when $|A|$ is sufficiently large. Evidently, the condition $|A| > |s(t)|$ is sufficient for guaranteeing the minimum phase property, as was originally reported in [15], and as we also demonstrate in Appendix A. When $h(t)$ is a minimum-phase signal, its phase $\phi(t)$ and absolute value $|h(t)|$ are uniquely related by the Hilbert transform:

$$\phi(t) = \frac{1}{\pi} \text{p.v.} \int_{-\infty}^{\infty} dt' \frac{\log[|h(t')|]}{t - t'}, \qquad (2)$$

where p.v. stands for *principal value*. Equation (2) is one of the two KK relations existing between ϕ and $\log[|h|]$, and it is most
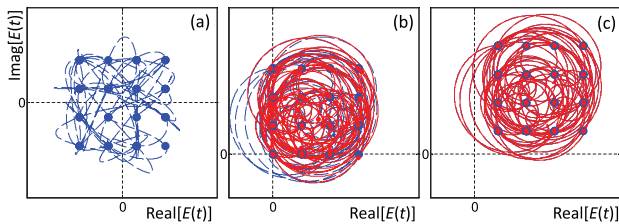

Fig. 1. (a) Time trajectory of a 16 QAM modulated signal $s(t)$ of bandwidth B in the complex plane. (b) The time trajectory of the single-sideband signal $A + s(t) \exp(-i\pi Bt)$ (blue dashed) and of the signal reconstructed from its intensity (red solid). We set the phase of A to 45° for the convenience of illustration. The blue and red dots are the original and reconstructed symbols, respectively. The quality of the reconstruction is poor because the original signal encircles the origin multiple times. (c) Same as (b), but with a larger value of $|A|$. Here the trajectory of the original signal does not encircle the origin, and the reconstruction is perfect.

conveniently implemented in the frequency domain, where it assumes the form

$$\tilde{\phi}(\omega) = i \, \text{sign}(\omega) \mathcal{F}\{\log[|h(t)|]\}, \qquad (3)$$

where $\text{sign}(\omega)$ is the sign function, which is equal to 1 for $\omega > 0$, to 0 for $\omega = 0$, and to -1 for $\omega < 0$, and where $\mathcal{F}$ denotes a Fourier transform. It should be noted that the phase reconstruction is exact up to a constant phase offset. This can be seen most easily from Eq. (3), where the zero-frequency component of $\tilde{\phi}(\omega)$ is set to zero by the sign function.

3. KK SCHEME

We proceed to describing the field reconstruction procedure performed by the KK receiver, where we assume for simplicity a scalar description of the field, and ignore, for the time being, fiber propagation effects. The treatment of vector fields follows trivially from applying the scalar description individually to each of the two orthogonal polarization components.

We denote the complex envelope of the incoming electric field by $E_s(t)$, which is assumed to be contained within a finite optical bandwidth denoted by B. The LO is assumed to be a continuous-wave (CW) signal whose amplitude is E_0 and whose frequency coincides with the left edge of the information-carrying signal spectrum. We assume that E_0 is real-valued and positive, which is equivalent to referring all phase values to that of the LO. The complex envelope of the field impinging upon the photo-diode is thus $E(t) = E_s(t) + E_0 \exp(i\pi Bt)$. The photocurrent I produced by the photodiode is proportional to the field intensity $I = |E(t)|^2$, where we have set the proportionality coefficient to 1, for the sake of simplicity. Assuming that E_0 is large enough to ensure that the signal $E(t) \exp(-i\pi Bt) = E_0 + E_s(t) \exp(-i\pi Bt)$ is minimum phase, Eqs. (2) and (3) can be used to reconstruct the signal $E_s(t)$ as follows:

$$E_s(t) = \left\{ \sqrt{I(t)} \, \exp[i\phi_E(t)] - E_0 \right\} \exp(i\pi Bt), \qquad (4)$$

$$\phi_E(t) = \frac{1}{2\pi} \text{p.v.} \int_{-\infty}^{\infty} dt' \frac{\log[I(t')]}{t - t'}. \qquad (5)$$

Note that the average value of the phase returned by Eq. (5) is zero, which implies the need for an additional phase-recovery procedure (as is customary in all coherent receivers).

A possible issue with the signal reconstruction described above is that the logarithm appearing in Eq. (5) introduces spectral broadening, which necessitates digital upsampling of the received photocurrent. An alternative signal reconstruction approach that resolves this issue is described in Appendix B. For the purpose of demonstrating the KK scheme, we assume in this paper that the upsampling of the photocurrent is not an issue, so in what follows we apply the procedure represented in Eqs. (2)–(5).

The implementation of the KK transceiver is plotted in Fig. 2(a). Figure 2(b) shows an alternative implementation, where the LO is added to the information carrying signal at the receiver using a frequency-selective coupler to avoid signal and LO loss. This implementation accommodates polarization multiplexing [19], eliminates the need for an optical hybrid at the receiver, and requires the use of a single photodiode. However, it is more costly as it requires a LO laser, and, hence, it is less suitable for short-reach links. When compared to balanced heterodyne, the KK scheme with the LO added at the receiver eliminates the need
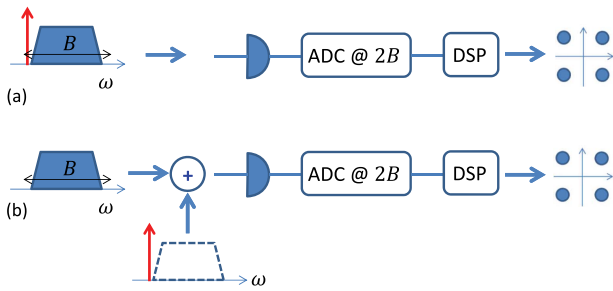
Fig. 2. (a) KK receiver scheme: the transmitted waveform, which consists of a modulated signal of bandwidth B and a CW field at the left edge of the signal spectrum, is directly detected, then sampled at the sampling rate of $2B$. The digital samples are finally processed for chromatic dispersion compensation and extraction of the transmitted symbols. (b) An alternative version of the KK scheme. In this case, the CW field at the left edge of the modulated signal spectrum is added at the receiver using a frequency selective coupler.

for balanced detection, whose implementation, especially at high baud rates, may become nontrivial. This benefit, however, is counterbalanced by a somewhat higher complexity of the post-detection processing. For this reason, in what follows we restrict ourselves to the first implementation of the KK scheme shown in Fig. 2(a), targeting short-reach transmission systems.

Since the bandwidth of the photocurrent I is twice larger than the bandwidth B of the optical signal, the minimum sampling rate that is required according to the Shannon–Nyquist sampling theorem is $2B$ [20]. The doubling of the bandwidth is consistent with the fact that the information that was previously encoded in a complex-valued signal is transferred by square-law detection into a real-valued signal without loss. The photocurrent samples are digitally upsampled, and then the natural logarithm operation is performed. The upsampling is required to accommodate the increase in bandwidth caused by the logarithm operation (digital upsampling by a factor of 3 is sufficiently accurate in the examples reported in what follows). A method for avoiding the need for upsampling is presented in Appendix B. Subsequently, a Hilbert transform is applied to obtain the phase ϕ_E and the complex signal $E_s(t)$, according to Eqs. (4) and (5). The upsampling, when implemented by means of zero-padding in the Fourier domain, requires a Fourier transform pair. Another Fourier transform pair is required by the Hilbert transform, so that the additional complexity implied by the KK scheme coincides with the complexity of two Fourier transform pairs. At this stage the signal $E_s(t)$ can be downsampled to the original sampling rate. The subsequent digital processing of the received signal is identical to the one that is found in standard coherent receivers, and is not detailed in the figure.

4. OPTIMALITY OF THE KK SCHEME

An important attribute of the KK scheme is that it is optimal in terms of information capacity with respect to the entire class of band-limited systems that are constrained to work with receivers that are only capable of detecting the signal's intensity. This optimality is demonstrated by two arguments. The first is that all minimum phase signals can be expressed in the form of Eq. (1), and communicated using the KK configuration. The second is that, of all signals with a given intensity waveform

in the time domain, the minimum phase signal is contained in the smallest bandwidth. The latter argument follows from the minimum-energy-delay property of minimum phase signals discussed in [21], with the only difference being that the time and frequency variables are interchanged [22]. The formal statement of this property is that the quantity $\int_{\omega_0}^{\infty} |\tilde{E}(\omega)|^2 d\omega$ is minimized when $\tilde{E}(\omega)$ is the Fourier transform of a minimum phase signal [23].

5. NUMERICAL VALIDATION OF THE KK RECEIVER

We start by providing a numerical proof-of-concept of the KK receiver scheme. To that end we consider the case in which the signal impinging upon the receiver is produced by filtering white Gaussian noise with a square optical filter of bandwidth B centered at $B/2$. Since Gaussian noise is characterized by the largest entropy that can be carried by signals of the same bandwidth, it seems natural to use it for validating the KK receiver concept.

Figure 3 shows the absolute values of the original and the reconstructed waveforms by solid and dashed–dotted lines, respectively (a similar picture corresponds to the real or imaginary parts). The computation was performed with $B = 32$ GHz, using a time window $T = 1024/B$. The signal samples used to perform the Hilbert transform were taken at a rate of $2B$. The signal used in the simulation was generated as a complex-valued circular Gaussian waveform with a flat-top spectrum of width $B = 32$ GHz, which was normalized such that its largest absolute value within the simulated time window was $0.99E_0$. The top panel shows the signal intensity within the entire simulated time window, whereas the bottom panels zoom into the waveform in two distinct intervals. In the left panel we show the beginning of the frame, where the edge effect of the Hilbert transform is visible. The waveform reconstruction error is visible initially, but then it reduces as the distance from the beginning of the frame increases. The waveform in the right panel is taken from the middle of the frame, where the edge effect is absent, and the quality of the reconstruction is excellent. As can be seen in the figure, the duration of the edge effect is of the order of 0.5 ns, which is
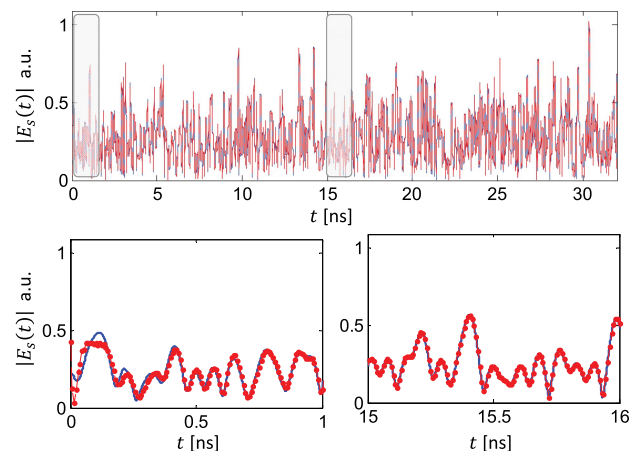

Fig. 3. Top panel shows the absolute values of the original (solid blue) and reconstructed (dashed red) waveforms. The bottom left and right panels zoom in to the beginning and the center of the frame, respectively.

equivalent to ∼16/B. The edges in the beginning and in the end of the processed frame will have to be discarded in a practical implementation of the KK receiver. A similar situation, where the edges of the processed frame need to be discarded, character-izes the digital compensation of chromatic dispersion.

6. LINEAR TRANSMISSION PERFORMANCE

We now switch to demonstrating the implementation of the KK transceiver in the context of a digital communication system transmitting quadrature amplitude modulation (QAM) signals. We focus first on the linear regime of operation, where the effect of the fiber nonlinearity is negligible.

Figure 4 refers to the back-to-back configuration. The panels show the received constellations for single-channel 16 QAM signaling, where a raised cosine fundamental waveform with 0.05 roll-off factor was assumed. Since this figure was plotted in the regime of linear transmission, and in the absence of noise, the displayed results are not affected by the baud rate. The various panels correspond to different settings of the LO power $P_{LO} = E_0^2$. In the leftmost panel, the LO power was set to 1.1 times the maximum value of the information-carrying signal power, corresponding to about 11 dB above the average signal power, and the received constellation was indeed perfect (the edge effect seen in Fig. 3 was taken care of by discarding the symbols at the edges of the simulation time window). In the re-maining three panels, the LO power level was reduced to 8, 6, and 3 dB above the average channel power. The figure shows that the received constellation quality deteriorates as the power of the LO is reduced. The scattering of the constellation points is caused by the fact that the instantaneous power of the information-carrying signal occasionally exceeds the LO power to an extent that it violates the minimum-phase condition required for signal reconstruction [15].

Practical considerations suggest that one should pick the low-est LO power for which the reconstruction noise shown in Fig. 4 is sufficiently small to allow reliable detection. Indeed, large values of the LO power would deteriorate the system's power efficiency and, as we show in the next section, reduce its tolerance to propagation-induced nonlinear distortions.

It should be stressed that, in spite of the multiple nonlinear operations required for signal reconstruction (square law detec-tion, logarithm, exponentiation, etc.), the KK receiver is a truly linear receiver for the class of minimum phase signals. In particu-lar, additive noise remains additive after reconstruction, as long as it does not cause violation of the minimum phase requirement. Such violation may occur either when the noise spectrum extends
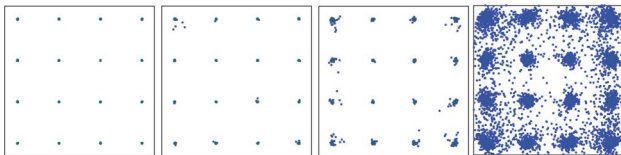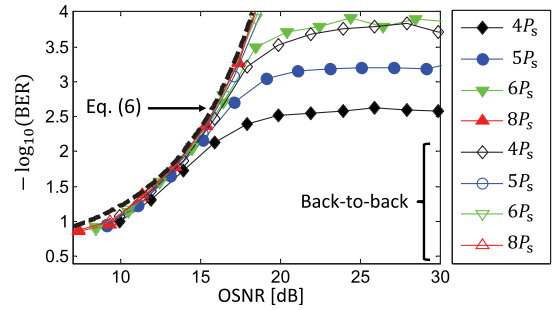

Fig. 5. BER versus OSNR for a 24 Gbaud 16 QAM modulated signal. Each curve was obtained by setting the power of the LO to the value shown in the legend. Open symbols refer to the back-to-back configu-ration, while the solid symbols were obtained for a 100 km single-span link, where CD was compensated electronically at the receiver after signal reconstruction.

to the left of the signal spectrum, or when its power is large to the extent that the condition discussed in Fig. 1 is not fulfilled. This property is quantitatively verified in Fig. 5, where we characterize the bit error rate (BER) of a KK receiver in the presence of am-plification noise for different values of the LO power. Plotted in the figure is the BER as a function of optical signal-to-noise ratio (OSNR) for a 24 Gbaud Gray-coded 16 QAM modulated signal, for a range of LO powers. Open symbols show the results ob-tained in the back-to-back configuration, whereas solid symbols refer to the case of *linear* transmission through a 100 km single-mode fiber link for which we assumed a chromatic dispersion coefficient of 21 ps^2/km, a loss coefficient of 0.22 dB/km, and an overall span loss budget of 26 dB. The OSNR was varied by varying the signal launch power. In the latter case, chromatic dispersion was compensated electronically at the receiver, after signal reconstruction. In all simulations, the information-carrying signal consisted of a pseudo-random sequence of 2^{15} symbols. Prior to reception, amplification noise was added to the signal and then a 12th-order super-Gaussian optical filter with a 3 dB bandwidth of 36 GHz was applied. The filter center frequency was set to 16.6 GHz above the LO frequency, higher than the center frequency of the data-carrying signal. This was done to reduce the amount of noise at lower frequency than the LO, while refraining from attenuating the LO. The dashed curve in the figure shows the plot of the approximate analytic expression for the BER of an M-QAM modulated system impaired by additive white Gaussian noise (AWGN). If we denote by ρ the ratio between the 0.1 nm bandwidth customarily used in the definition of the OSNR and the information-carrying signal bandwidth, this reads [24]

$$\text{BER}_{\text{AWGN}} = \frac{4}{\log_2(M)}\left(1 - \frac{1}{\sqrt{M}}\right)Q\left(\sqrt{\frac{6\rho}{M-1}\text{OSNR}}\right), \quad (6)$$

where $Q(x) = (1/2)\text{erfc}(x/\sqrt{2})$. This figure shows that, with a sufficiently large LO power, the BER in the linear regime coin-cides with the BER obtained by an ideal coherent receiver, quan-titatively validating the fact that the KK receiver behaves as an ideal coherent receiver for the class of minimum phase signals. This property is in striking contrast with other direct detection techniques like PAM, where square law detection introduces a correlation between the noise and the detected signal, which

Fig. 4. Received constellations in the back-to-back configuration. In the leftmost panel, the LO power was set to 1.1 times the maximum value of the information carrying signal power—corresponding to about 11 dB above the average signal power. In this case, the minimum-phase condition [15,16] is rigorously fulfilled. In the second, third, and fourth panels, the LO power level was reduced by 3, 5, and 8 dB, respectively, while not modifying the signal.

Table 1. Comparison among Various Schemes in Terms of Optical Bandwidth, Suitability for Digital Compensation of Linear Impairments, and Power Efficiency[a]

	Optical Bandwidth	Digital Compensation	P_{LO}/P_s
IMDD	R	not possible	N/A
Self-heterodyne [4]	R	possible	~1
Ref. [6]	$R/2$	not possible	≫1
Ref. [7]	$R/2$	possible	≫1
KK	$R/2$	possible	>1

[a]The symbol R represents the bandwidth of the detected photocurrent, which is also the lowest acceptable sampling rate. The ratio P_{LO}/P_s ranges from 10 to 20 in [6], and is of the order of 30 in [7]. This ratio reduces to values ranging from 4 to 8 in the case of the KK scheme.

should be properly taken into account in both receiver design and performance estimation.

The figure confirms the benefit of increasing the LO power: at low levels the BER saturates for increasing OSNR, owing to the errors caused by imperfect signal reconstruction. This saturation tends to disappear when the LO power is sufficiently large. The difference between the back-to-back results and the results obtained after transmission through a single-mode fiber (SMF) shows that electronic chromatic dispersion (CD) compensation implies an OSNR penalty, as well as an increase in the smallest achievable BER. The reason for this penalty is in the larger peak-to-average power ratio (PAPR) of the CD-impaired information-carrying signal, as compared to the PAPR of the launched signal. The OSNR penalty could in principle be avoided either by pre-compensating the modulated signal, or by implementing *optical* CD compensation at the receiver, although this would imply an obvious complication of the transceiver structure.

The simulation results of Fig. 5 indicate that, for OSNR values higher than ~16 dB, pre-forward error correction (FEC) BERs lower than 10^{-2} can be achieved with a local oscillator power exceeding the average channel power by about 6 dB (implying that the total transmit power increases by 7 dB relative to coherent transmission). This makes the KK scheme considerably more power efficient than the scheme proposed recently in [7], but less efficient than intensity-modulation direct-detection (IMDD) and self-heterodyne [4,5]. On the other hand, it should be stressed that the KK scheme is twice more spectrally efficient than IMDD [25] and the self-heterodyne scheme. A detailed comparison with other known direct-detection schemes in terms of spectral efficiency, power efficiency, and amenability to digital dispersion compensation is shown in Table 1. To facilitate the comparison of spectral efficiencies, we express the optical bandwidth in terms of R, which is the lowest sampling rate that allows reconstruction of the detected photocurrent [26]. As can be seen from the table, the KK scheme provides an attractive combination of properties.

7. NONLINEAR TRANSMISSION PERFORMANCE

In this section we investigate the limitations imposed by the fiber nonlinearity to the implementation of the KK transceiver in coherent transmission systems of the kind considered in the previous section. The main results of this investigation are presented in Figs. 6 and 7, which were obtained for a dense wavelength
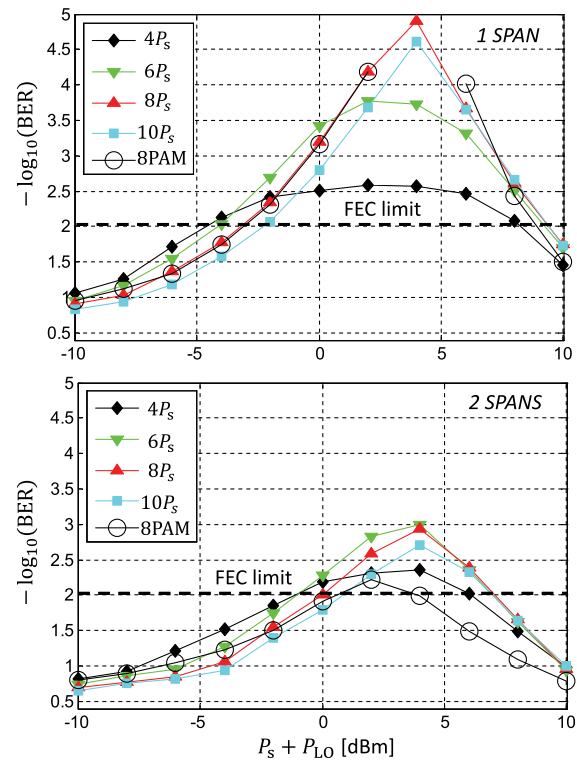

Fig. 6. BER versus total transmit power for the channel of interest of a DWDM system with five transmitted channels. The solid symbols were obtained for 16 QAM modulation based on the use of the KK scheme with various levels of the LO power; the open circles show the results obtained for 8 PAM modulation. In the KK scheme CD was compensated digitally after signal reconstruction, whereas in the case of 8 PAM, CD was compensated optically. Top and bottom panels differ by the number of spans.

division multiplexing (DWDM) system with five 16 QAM channels at 24 Gbaud. The channel spacing was set to 40 GHz, and the simulations were again performed with a random sequence of 2^{15} symbols, so that the computed BER is accurate up to values of the order of 10^{-4}. The BER of the channel of interest is plotted in Fig. 6 as a function of the total transmit power, which is the sum of the channel power and the LO power. The top panel and the bottom panel refer to a one-span and a two-span system, respectively, where in both cases a standard SMF was assumed with a nonlinearity coefficient of 1.3 km^{-1} W^{-1}. Here, too, the various curves correspond to different values of the LO power, and CD was compensated digitally after signal reconstruction. As can be seen in the top panel of Fig. 6, the FEC threshold of 10^{-2} is exceeded for a broad range of power levels. As expected, the BER improves with the launched power, until it reaches an optimal value, after which it deteriorates as a result of growing nonlinear distortions. The effect of the LO power is dual. On the one hand, it improves compliance with the minimum-phase condition, which is beneficial for the BER. On the other hand, it enhances the nonlinear distortion, whose effect on the BER is adverse. For this reason, the dependence of the peak BER on the LO power is not monotonic. In the single-span case, the peak BER improves by increasing the LO power from 6 dB ($P_{LO} = 4P_s$) to 9 dB ($P_{LO} = 8P_s$), and then it deteriorates when the LO power is raised beyond 9 times the average power of the data-carrying
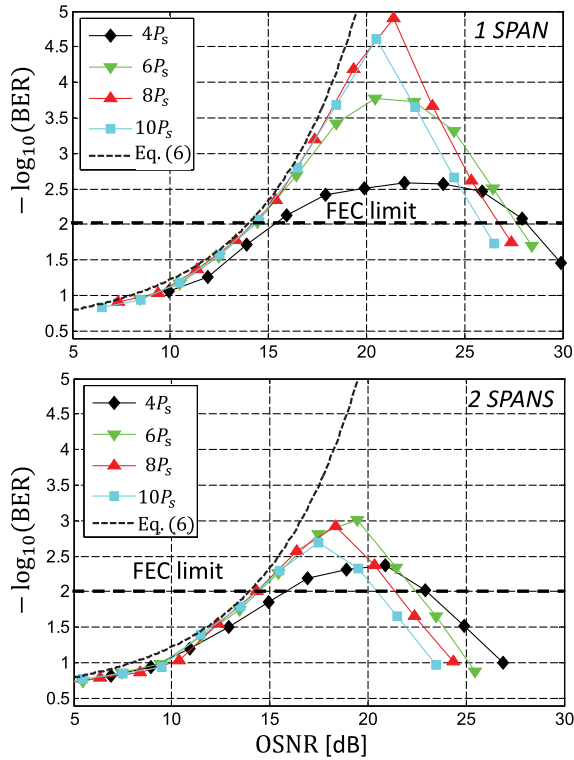
Fig. 7. Same as Fig. 6, except that the BER is plotted versus the OSNR. At low OSNR values, increasing the LO power yields a reduction in BER.

signal. A similar behavior is seen in the two-span case. In parallel, the range of channel powers for which the FEC requirement is satisfied shrinks fairly monotonically with increasing LO power.

For comparison we show in the same figure the BER of an 8 PAM system operated at the baudrate of 32 Gbaud, so as to provide the same throughput. In this case the channel spacing was set to 50 GHz, and optical CD compensation was implemented at the receiver. The fundamental waveform used was the same as in the case of 16 QAM modulation, and eight equally spaced *amplitude* (not intensity) levels were used to encode the information. No substantial difference in performance between the two schemes is seen in the single-span case, whereas in the two-span configuration the KK scheme outperforms PAM (even considering the idealized implementation of 8 PAM that we simulated in this work). In addition, we remind the reader that the performance of 16 QAM comes with a spectral occupancy smaller by two-thirds than that of 8 PAM.

We stress that in Fig. 6 the BER is plotted as a function of the total power $P_s + P_{LO}$, and, therefore, curves obtained for higher LO powers correspond to lower signal powers and lower OSNR. This should not be misconstrued as implying that the decrease of the LO power is beneficial, which would contradict the results of Fig. 5. The apparent contradiction disappears when the BER values of Fig. 6 are shown as a function of the OSNR (which is proportional to the signal power P_s for a given noise power), as done in Fig. 7. The dashed curves in the two panels show the plot of the BER expression given in Eq. (6). Inspection of Fig. 7 shows that the dependence of the BER on the OSNR in the linear regime is almost identical in all curves, with a deviation for the smallest value of the local oscillator power, where the BER is

slightly higher because the error probability caused by the non-compliance with the minimum-phase condition becomes of the order of the BER caused by the AWGN. It also shows that Eq. (6) appears to provide an excellent approximation of the BER curves in the linear regime of operation. These results are consistent with the results in the linear regime presented and discussed in Section. 6.

8. CONCLUSIONS

We proposed and demonstrated numerically a direct-detection receiver scheme for coherent communications. The principle underpinning of the proposed receiver is based on the famous KK relations, while its implementation requires transmitting a CW signal at one edge of the information-carrying signal. The KK receiver allows full reconstruction of the received complex signal from the detected photocurrent and, hence, the digital compensation of chromatic dispersion. We showed that the KK receiver favorably compares to existing schemes in terms of power consumption and is optimal in terms of spectral efficiency.

APPENDIX A: PROOF OF THE SUFFICIENT MINIMUM-PHASE CONDITION

The necessary and sufficient condition that characterizes minimum-phase signals follows from the Nyquist criterion, as described in [16]. A sufficient condition was derived in [15], and we prove it here in a way that relates more directly to the setup considered in this paper.

In the case of a single-sideband signal $u(t) = u_r(t) + iu_i(t)$, the real and imaginary parts $u_r(t)$ and $u_i(t)$ are related through the KK relations. A straightforward way to see this is based on expressing its Fourier transform $\tilde{u}(\omega)$ as $\tilde{u}(\omega) = (1/2)[1 + \text{sign}(\omega)]\tilde{u}(\omega)$, which follows from the single-sideband condition $\tilde{u}(\omega) = 0$ for all $\omega < 0$. Using integration by parts together with the fact that the inverse Fourier transform of sign (ω) is $-i/(\pi t)$, it follows that $u(t) = u(t)/2 + i\text{p.v.} \int_{-\infty}^{\infty} dt' u(t')/[2\pi(t - t')]$, that is $u(t) = i\text{p.v.} \int dt' u(t')/[\pi(t - t')]$, from which the famous KK relations [10,11] follow:

$$u_r(t) = -\text{p.v.} \int_{-\infty}^{\infty} \frac{u_i(t')dt'}{\pi(t - t')},$$

$$u_i(t) = \text{p.v.} \int_{-\infty}^{\infty} \frac{u_r(t')dt'}{\pi(t - t')}. \qquad \textbf{(A1)}$$

Let us now define $1 + u(t) = |1 + u(t)| \exp[i\varphi(t)]$ and consider the function $U(t) = \log[1 + u(t)] = \log|1 + u(t)| + i\varphi(t)$. The terms $|U(t)| = \log|1 + u(t)|$ and $\varphi(t)$ are the real and imaginary parts of the new function $U(t)$. In what follows, we demonstrate that the condition $|u(t)| < 1$ guarantees that $U(t)$ is single sideband, and hence $|U(t)|$ and $\varphi(t)$ are also related through KK relations identical to Eq. (A1).

With the condition $|u(t)| < 1$ for all t, we may expand $U(t) = \log[1 + u(t)] = \sum_{n=1}^{\infty} (-1)^{n+1} u^n(t)/n$. Since the spectrum of $u^n(t)$ is the nth order autoconvolution of $\tilde{u}(\omega)$, it is zero for $\omega < 0$ and, hence, the spectrum of $U(t)$ is single sideband (i.e., it is zero for all $\omega < 0$), thereby implying the equality

$$\varphi(t) = \text{p.v.} \int_{-\infty}^{\infty} dt' \frac{\log|1 + u(t')|^2}{2\pi(t - t')}. \qquad \textbf{(A2)}$$

Defining $E_s(t) = E_0 u(t)$, where E_0 is a real positive quantity, and using the fact that p.v. $\int dt' \log(E_0^2)/[2\pi(t - t')] = 0$, we obtain

$$\phi_E(t) = \text{p.v.} \int_{-\infty}^{\infty} dt' \frac{\log|E_0 + E_s(t)|^2}{2\pi(t - t')}, \qquad \textbf{(A3)}$$

where, by substituting $I(t) = |E_0 + E_s(t)|^2$, Eq. (5) is obtained. Equation (A3) states that $\phi_E(t)$ is the Hilbert transform of $\log[I(t)]$.

APPENDIX B: ITERATIVE SIGNAL RECONSTRUCTION WITHOUT UPSAMPLING

An alternative signal reconstruction approach that avoids the need for upsampling makes use of the fact that the frequency shifted signal $E_s'(t) = E_s(t) \exp(-i\pi Bt)$ has real and imaginary parts $E_{s,r}'(t)$ and $E_{s,i}'(t)$, satisfying the KK relations

$$E_{s,i}'(t) = \frac{1}{\pi} \text{p.v.} \int_{-\infty}^{\infty} dt' \frac{E_{s,r}'(t')}{t - t'}. \qquad \textbf{(B1)}$$

By using $I(t) = |E_0 + E_s'(t)|^2$, one obtains the equality

$$I(t) = E_0^2 + E_{s,r}'^2(t) + E_{s,i}'^2(t) + 2E_0 E_{s,r}'(t). \qquad \textbf{(B2)}$$

Once $E_{s,i}'(t)$ is replaced by its expression given by Eq. (B1), Eq. (B2) becomes an integral equation that, being equivalent to Eqs. (4) and (5), has only one solution satisfying the minimum-phase condition [16]. This solution can be obtained by means of the procedure described in what follows, and which does not require upsampling. Equation (B2) can be formally solved for $E_{s,r}'(t)$ with the result

$$E_{s,r}'(t) = \sqrt{|I(t) - E_{s,i}'^2(t)|} - E_0, \qquad \textbf{(B3)}$$

where we have taken the positive determination of the square root because it is the only one consistent with the minimum-phase condition. The absolute value in the argument of the square root was added to ensure that $E_{s,r}'(t)$ remains real-valued during the iteration process. Equation (B3) can be solved by multiple iterations, where in the first step one solves for $E_{s,r}'(t)$ while setting $E_{s,i}'(t) = 0$ on the right-hand side of Eq. (B3). The resulting $E_{s,r}'(t)$ is then used to extract the next iteration of $E_{s,i}'(t)$ through Eq. (B3). The procedure is then repeated until the values of $E_{s,r}'(t)$ and $E_{s,i}'(t)$ stabilize. At the end of each iteration, the reconstructed field $E_s'(t) = E_{s,r}'(t) + iE_{s,i}'(t)$ is digitally filtered by a square filter of passband $(0, B]$, so as to remove out-of-band spectral components produced by the square-root operation. Within this procedure, the samples of the photocurrent $I(t)$ used in Eq. (B3) are taken at the rate of $2B$, and, therefore, no upsampling is needed. An estimate of the error implied by the iterations can be gained by looking at the time average of the absolute value of the difference between the measured intensity $I(t)$ and that obtained from the reconstructed field $|E_0 + E_s'(t)|^2$, normalized to $|E_0|^2$. In all cases considered in this work, relative errors of about 1%, which are acceptable for relevant system applications, are obtained with up to three iterations only. The accuracy increases with the number of iterations implying stability of the algorithm, with faster convergence for larger values of the LO power.

REFERENCES AND NOTES

1. S. Randel, F. Breyer, S. C. J. Lee, and J. W. Walewski, "Advanced modulation schemes for short-range optical communications," IEEE J. Sel. Top. Quantum Electron. **16**, 1280–1289 (2010).
2. T. Takahara, T. Tanaka, M. Nishihara, Y. Kai, L. Li, Z. Tao, and J. Rasmussen, "Discrete multi-tone for 100 Gb/s optical access networks," in *Optical Fiber Communication Conference*, OSA Technical Digest (online) (Optical Society of America, 2014), paper M2I.1.
3. A. Weiss, A. Yeredor, and M. Shtaif, "Iterative symbol recovery for power efficient DC biased optical OFDM systems," J. Lightwave Technol. **34**, 2331–2338 (2016).
4. A. J. Lowery and J. Armstrong, "Orthogonal-frequency-division multiplexing for dispersion compensation of long-haul optical systems," Opt. Express **14**, 2079–2084 (2006).
5. B. J. C. Schmidt, A. J. Lowery, and J. Armstrong, "Experimental demonstrations of electronic dispersion compensation for long-haul transmission using direct-detection optical OFDM," J. Lightwave Technol. **26**, 196–203 (2008).
6. M. Schuster, S. Randel, C. A. Bunge, S. C. J. Lee, F. Breyer, B. Spinnler, and K. Petermann, "Spectrally efficient compatible single-sideband modulation for OFDM transmission with direct detection," IEEE Photon. Technol. Lett. **20**, 670–672 (2008).
7. S. Randel, D. Pilori, S. Chandrasekhar, G. Raybon, and P. J. Winzer, "100-Gb/s discrete-multitone transmission over 80-km SSMF using single-sideband modulation with novel interference-cancellation scheme," in *Proceedings of European Conference of Optical Communications 2015 (ECOC)*, Valencia, Spain (2015), paper 0697.
8. Toward the completion of this paper, we discovered that a similar scheme was proposed in Ref. [9]. That scheme was presented in the context of analog radio systems and it contained none of the features that characterize fiber-optic transmission, which are discussed in this paper.
9. H. Voelcker, "Demodulation of single-sideband signals via envelope detection," IEEE Trans. Commun. Technol. **14**, 22–30 (1966).
10. R. L. Kronig, "On the theory of the dispersion of x-rays," J. Opt. Soc. Am. **12**, 547–557 (1926).
11. H. A. Kramers, "La diffusion de la lumiere par les atomes," Atti Cong. Intern. Fis. **2**, 545–557 (1927).
12. M. Cini, "The response characteristics of linear systems," J. Appl. Phys. **21**, 8–10 (1950).
13. M. Gell-Mann and M. L. Goldberger, "The formal theory of scattering," Phys. Rev. **91**, 398–408 (1953).
14. W. Heisenberg, "Quantum theory of fields and elementary particles," Rev. Mod. Phys. **29**, 269–278 (1957).
15. A. Mecozzi, "Retrieving the full optical response from amplitude data by Hilbert transform," Opt. Commun. **282**, 4183–4187 (2009).
16. A. Mecozzi, "A necessary and sufficient condition for minimum phase and implications for phase retrieval," arXiv:1606.04861 (2016).
17. Y. Shechtman, Y. C. Eldar, O. Cohen, H. N. Chapman, J. Miao, and M. Segev, "Phase retrieval with application to optical imaging: a contemporary overview," IEEE Signal Process. Mag. **32**(3), 87–109 (2015).
18. H. W. Bode, *Network Analysis and Feedback Amplifier Design* (Van Nostrand, 1945), Chap. 8.
19. Polarization multiplexing can also be accommodated by the scheme of Fig. 2(a), but envisageable extensions of the KK scheme would imply a considerable increase of the receiver cost and complexity.
20. We note that B represents the bandwidth of the optical signal impinging upon the receiver, which is meant to be reconstructed. The information-carrying bandwidth may be smaller than B, depending on the tightness of the optical filter that is used.
21. A. V. Oppenheim, R. W. Schafer, and J. R. Buck, *Discrete-Time Signal Processing* (Prentice Hall, 1999).

22. Recall that, contrary to [21] and to most of the existing literature, we are considering signals that are "causal" in the frequency domain, i.e., such that they vanish for $\omega < 0$.

23. To see why the minimum energy-delay property implies that of all signals with the same intensity profile, the minimum phase signal is contained within the smallest bandwidth, consider the following situation. Assume that $E(t)$ is a minimum phase signal, whose spectrum $|\tilde{E}(\omega)|^2$ is contained in the bandwidth B, but exceeds any bandwidth $B' < B$. If there were a signal $E'(t)$ such that $|E'(t)|^2 = |E(t)|^2$, with a spectrum $|\tilde{E}(\omega)|^2$ that is contained in $B' < B$, then we would have $\int_{\omega_0}^{\infty} |\tilde{E}(\omega)|^2 \mathrm{d}\omega > \int_{\omega_0}^{\infty} |\tilde{E}'(\omega)|^2 \mathrm{d}\omega = 0$ for every $\omega_0 \in (B', B)$, contrary to the minimum energy-delay property.

24. J. G. Proakis, *Digital Communications*, 4th ed. (McGraw-Hill, 2001), Chap. 5.

25. The lower spectral efficiency of IMDD follows from the fact that, with intensity modulation, no information is encoded into the optical phase. This makes IMDD inferior even to single-quadrature modulation, where positive and negative amplitude values can be used.

26. The rate R is in general different from the actual sampling rate. For instance, in the experimental implementation of the scheme of [4] presented in [5], the sampled photocurrent includes the contribution of the spurious signal–signal beat, which is filtered out in the digital domain, so that the minimum sampling rate is $2R$. In addition, in most practical implementations, the sampling rate is equal to twice the symbol rate, and hence it is higher than R.